International Journal of Chemical Studies

P-ISSN 2349–8528
E-ISSN 2321–4902
IJCS 2014; 2(5): 39-45

Received: 30-12-2014
Accepted: 01-03-2015

Abdullah A. Hussein
Department of Material Science, Polymer Research Centre, University of Basrah, Iraq

Waleed A. Hussain
Department of physics, college of education, Basrah University, Iraq

Hussein F. Al-luaiby
Department of physics, college of education, Basrah University, Iraq

Correspondence:
Abdullah A. Hussein
Department of Material Science, Polymer Research Centre, University of Basrah, Iraq

Performance enhancement of P3HT:Fullerene solar cells by varying weight ratios

Abdullah A. Hussein., Waleed A. Hussain and Hussein F. Al-luaiby

Abstract
Gold nanoparticles (AuNPs) deposited at the interface of the hole-collecting buffer layer [poly(3,4ethylenedioxythiophene):poly(styrenesulfonate) (PEDOT:PSS)] and regioregular poly(3-hexylthiophene):[6,6]-phenylC61-butyricacidmethylester (rr-P3HT): (PCBM) active layer were found to significantly increase organic solar cell performance. Organic solar cell devices were fabricated with weight ratio 1:0.7, 1:0.8, 1:0.9 and 1:1. of P3HT and PCBM, respectively. The photo-physical properties of these devices with varying weight ratios are investigated. We find that, absorption spectrum of the blend becomes broad with ratio varying, which is highly desirable for an organic solar cell devices. Film morphology is evaluated by atomic force microscopy (AFM). XRD patterns and External quantum efficiency (EQE) Measurements are also performed for the best device. The efficiency enhancement for the device with 1:1 is more significant than for 1:0.9, 1:0.8 and 1:0.7 weight ratios of P3HT and PCBM. With varying weight ratios, the solar cells upon (1:1) give Power Conversion Efficiency (PCE) of 3.01%, in contrast to 2.6% for (1:0.9), 2.01% for (1:0.8) and % 1:0.7 devices.

Keywords: Green synthesis of Silver nanoparticles by using orange extract.

1. Introduction
Converting solar energy into electrical energy is becoming significant because the crisis in conventional energy sources nowadays. There are different natural resources available to generate energy. Converting solar energy into electrical energy is one of such exploitation of the natural sources. Inorganic solar cells are the best utilized for the last few decades in this direction. But, the drawbacks such as manufacturing high costs and difficult fabrication process made researchers to look into easily processable nature and low cost polymer materials. Much work has been done for almost last one decade on polymer solar cells, but the lower power conversion efficiency (PCE) limits their commercial usage [1–10]. After introduction of bulk-heterojunction concept, the PCE of polymer solar cells is nearing to 5% [7–10]. But, these values are not sufficient to meet realistic specifications for commercialization.
The formation of bulk-heterojunction phase allows for bulk separation of photoinduced excitons and high-mobility removal of electron through the nano-phase. Poly(3-hexylthiophene) (P3HT) has been the mostly used p-type material [7–10] in polymer solar cells along with a fullerene derivative, [6,6]-phenyl C61- butyric acid methyl ester (PCBM) as an electron acceptor. Since hole is typically the high-mobility carrier in regioregular P3HT [11], the enhanced electron mobility was achieved by addition of electron acceptor. However, the difficulty in these systems arises when we account for the effects of morphological modifications in P3HT phase due to the introduction of nano-phase [1, 12]. There are significant number of studies that investigate the effects of processing parameters on blended photoactive nano-phase [12–16]. Even, the regioregularity and molecular weight [17, 18] of P3HT also affect the performance of P3HT:PCBM devices.
The electric power extracted from a photovoltaic device depends on both the photocurrent and photovoltage of the diode under illumination of a given intensity. In order to increase the PCE of a photovoltaic device, the practicable approach is to increase the photocurrent as much as possible, since the solar cell is limited by the built-in potential and it is the difference between the highest occupied molecular orbital (HOMO) and lowest unoccupied molecular orbital (LUMO) of the electron donor and acceptor materials [19]. Different device geometries and interface morphologies are evaluated for the purposes of trapping more light, dissociating excitons more efficiently, transporting charges with fewer impediments in order to extract more photocurrent [20].

Indeed, the solvents used for the preparation of active layer have shown a strong impact on its morphology, which influences the generation of photocurrent in the devices [15, 16]. Unfortunately, till to date no conclusive result was made for optimal processing of the nanophase.

2. Experiment

2.1. Photovoltaic device fabrication

Pre-patterned indium tin oxide (ITO)-coated glass slides (80 nm thick, 10Ω/sq sheet resistance). The ITO substrates were first cleaned with ultrasonicated in acetone and isopropyl alcohol for 10 min, heat dried in an oven at 120 ^{0}C and finally treated by ozone–ultraviolet cleaner for 10 min. The gold nanoparticles AuNPs were added to linear polystyrene (PS) in order to inhibit the dewetting in the spun-cast films. The PS acts as an inert host to improve the film forming property of the AuNPs [10]. The AuNPs solution was prepared by mixing the AuNPs with the PS (1:4 w/w) into the toluene solvent. A film of poly(ethylene dioxythiophene) (PEDOT: PSS:AuNPs) was spin cast on top of the ITO substrates with a speed of 2000 r/min for 40 s to form the hole- transport layer, and was dried for 15 min at 140 ^{0}C. Afterwards, the mixed solutions consisting of P3HT (10 mg mL^{-1}, Sigma-Aldrich) and PCBM (`10 mgmL^{-1}, Sigma-Aldrich) in co-solvent by mixing chlorobenzene and chloroform (CB:CF) solvent in 1:1 weight ratio were spin cast in a nitrogen-filled glove-box, then spin-coated at 800 rpm on the PEDOT:PSS film to form the active layer. The thickness of the active layer is ~150 nm and thickness of the PEDOT:PSS layer (30 nm) . Finally, a bilayer cathode consisting of 100 nm Al was thermal evaporated under high vacuum of ~ 2×10^{-5} Pa with a rate of 0.2 nm/s onto the polymer layer as a cathode to create a device with an active area of 9 mm^2 defined by a shadow mask on the active layer to form cells with an active area of 1 cm^2. The schematic diagram of the device structure is shown in Fig.1.

2.2 Device characterization

The current density–voltage (J–V) characteristics of devices were measured with a computer-programmed Keithley 2400 Digital SourceMeter and the photocurrent was generated under AM 1.5 G irradiation of 100 mWcm^{-2}. P3HT:PCBM films were prepared by spin coating P3HT:PCBM solution on glass substrates for UV–vis absorption spectroscopy and atomic force microscopy (AFM).The UV–vis absorption spectra of the polymer films were taken with a Varian Cary 5000UV–VIS–NIR spectrometer and Raman spectroscopy using a Horiba Jobin Yvon HR800 micro-Raman spectrometer. The light intensity for the solar simulator was calibrated with a standard photovoltaic (PV) reference cell. Incident photon to electron conversion efficiency (IPCE) curves were measured with a Stanford lock-in amplifier 8300 unit. The AFM images of the polymer films were acquired using a BRUKER NanoScope IV Multi-Mode Adapter AFM with the tapping mode. The film thickness was determined with aTencorP-10 Alpha-Stepprofiler.

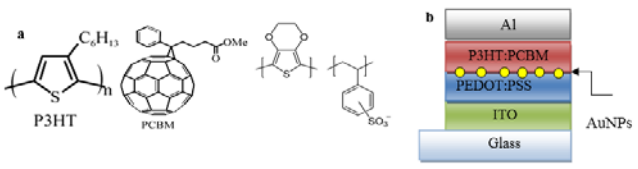

Fig 1: (a) Molecular structures of PEDOT:PSS:AuNPs /P3HT: PCBM (b) photovoltaic device structure.

The PCE (g) is described by g = FF× (Voc × Jsc)/P_{light}, where the FF is defined as FF= (Imax × Vmax)/(Isc× Voc) and the P_{light} is the power of incident light. The PCEs of the pristine and hybrid OSCs were estimated for AuNPs.

3. Results and Discussion

The UV–vis absorption spectra of PEDO:PSS:AuNPs /P3HT:PCBM films with different weight PCBM:P3HT active layer ratios 1:0.7, 1:0.8, 1:0.9 and 1:1.,in the range from 300 nm to 800 nm, are shown in Fig. 1. It is clearly shown that the absorption spectrum of the blend becomes broad with ratio varying, which is highly desirable for an organic solar cell devices. The varying PCBM:P3HT active layer ratios films showed varying absorption intensities and locations because the P3HT and PCBM had different absorption positions, and they were mixed in different ratios. The absorption intensities of the films increased with the increase of PCBM:P3HT active layer ratio from 1: 0.7 to 1:1 because the P3HT molecular had a stronger absorption in visible light region by π-π* interaction of the P3HT molecules [20]. However, when the ratio was decreased to 1:0.7, the absorption intensity decreased, which was attributed to the uneven distribution of the P3HT in the blend. So, the film with PCBM:P3HT active layer ratio at 1:1 had the highest absorption intensity, which is an significant factor in enhancing the photoelectric performance of the solar cell.

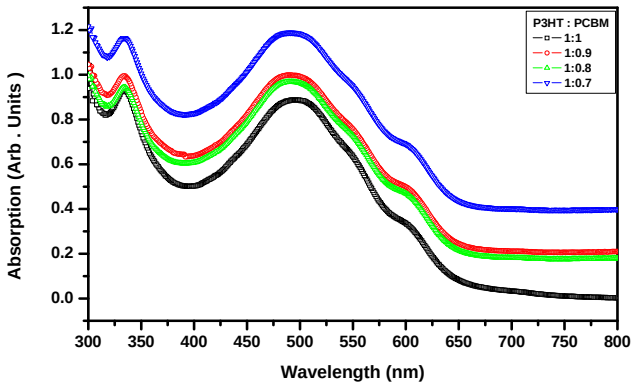

Fig 2: UV–vis absorption spectra of PEDOT:PSS:AuNPs/P3HT:PCBM films with different weight ratios 1:0.7, 1:0.8, 1:0.9 and 1:1.

The XRD patterns of PEDO:PSS:AuNPs /P3HT:PCBM films with different weight PCBM:P3HT active layer ratios 1:0.7, 1:0.8, 1:0.9 and 1:1, are shown in Fig. 3. For all of the prepared P3HT:PCBM active layers, a characteristic (corresponds to the first-order reflection peak →100) peak around 2θ=5.4^o representing the oriented edge-on P3HT crystallites with the lamella structure of thiophene rings in P3HT [22] has grown up significantly with 1:0.7, 1:0.8, 1:0.9, and 1:1 respectively, and its half width has decreased. This indicates the increase in the degree of crystallization and/or the grain size of P3HT domains by 1:1 ratio. The ratios 1:0.8 and 1:0.9 films show a reduced intensity of (100) peak as compared to that of the ratio 1:1film. The lowest crystallinity was observed for the as deposited 1:0.7 film. We assume that the presence of PCBM molecules affect the structure of P3HT crystallites at room temperatures. Upon ratio 1:1, the significant increase in P3HT crystallinity can be ascribed to the full self-assembly of the conjugated chain leading to the orderly formed and increased length of the conjugated bond. This is due to the increased homogeneous diffusion of PCBM

molecules at elevated temperatures to form larger PCBM aggregates [23]. As a result, regions with low PCBM concentration will occur. In these regions with low PCBM concentration (phase-separated networks), the P3HT aggregates form larger crystallites and thus facilitates charge transport to the electrodes [24].

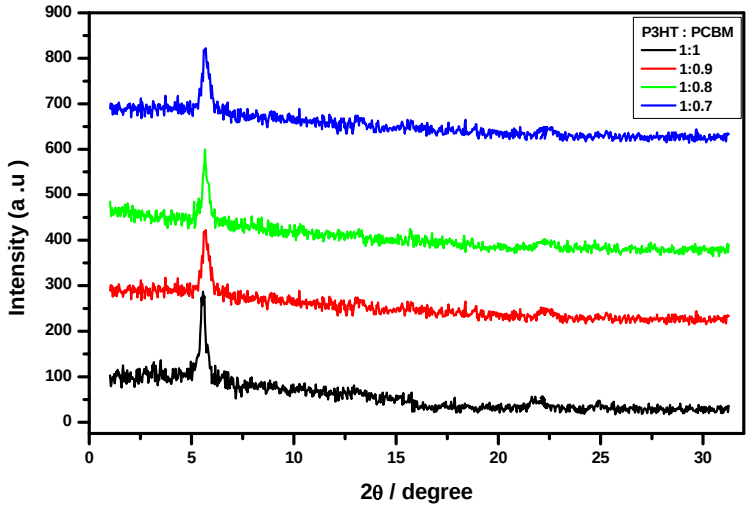

Fig 3: XRD curves of PEDOT:PSS:AuNPs/P3HT:PCBM films with different weight ratios 1:0.7, 1:0.8, 1:0.9 and 1:1.

The Raman spectroscopy of PEDO:PSS:AuNPs /P3HT:PCBM films with different weight PCBM:P3HT active layer ratios 1:1, 1:0.9, 1:0.8 and 1:0.7 , deposited on a Al substrate, are shown in Fig. 4. It was characterized by Raman spectroscopy in the range 200-2000 cm^{-1}. There are several Raman modes in the range 600-1600 cm^{-1} [25, 26] The spectrum of the blend deposited on Al features all the vibrational frequencies expected for the organic conjugated polymer [27]. The main in-plane ring skeleton modes at 1452 – 1468 cm^{-1} (symmetric C=C stretching mode) and at 1381-1391 cm^{-1} (C-C intra-ring stretching mode), the inter-ring C-C stretching mode at 1200-1210 cm^{-1}, the C-H bending mode with the C-C inter-ring stretch mode at 1180-1200 cm^{-1}, and the C-S-C deformation mode at 720-740 cm^{-1}. We focus on the two main in-plane ring skeleton modes at ~1450 and ~1380 cm^{-1}, because they are supposed to be sensitive to π-electron delocalization (conjugation length) of P3HT molecules [28] as well as to crystallinity extent [29, 30]. It is observed that the downward shift in the wavenumber generally indicates an increase in the crystallinity of P3HT polymer and the extension of the effective conjugation length along the polymer backbone [31]. The intensity and the full width at half maximum (FWHM) of P3HT and its blends of the C=C stretching deformation are often used as an indication of the ordering in the material. The P3HT polymer film prepared with a PCBM has the favourable molecular morphologies for the transport of charge carriers and is also responsible in the improvement of cell efficiencies. No Raman modes features attributable to PCBM, such as the A_{1g}1469 cm^{-1} mode of fullerenes could be resolved. Huang YC [31] showed that the Raman modes of P3HT polymer in the blends are not influenced by the contributions of the PCBM fluorescence. The results obtained from the Raman spectra, by suggesting that an increase in the P3HT:PCBM blend ratio reduces the effective conjugated polymer length of the polymer backbone and hence the order within the polymer. As a result, the polymer film prepared with P3HT:PCBM weight ratio of 1:1 has favourable molecular morphologies for transport of charge carriers and hence improved cell efficiencies.

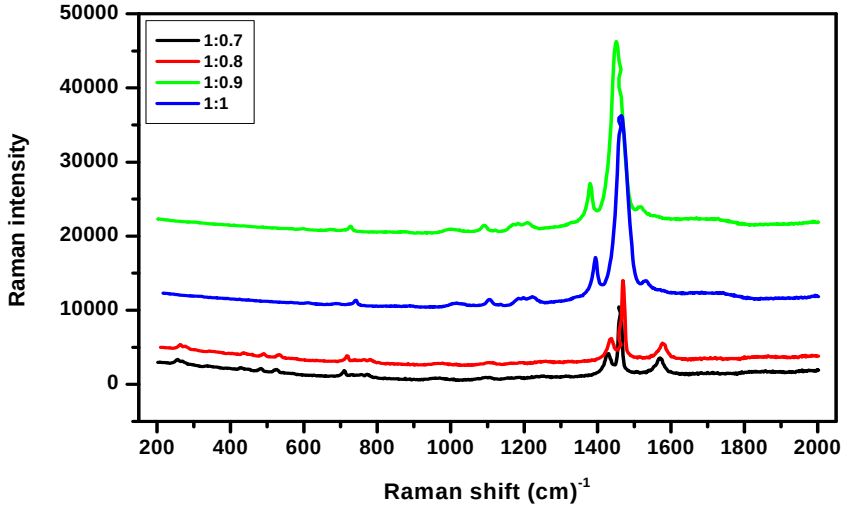

Fig 4: Raman spectroscopy for PEDOT:PSS:AuNPs/P3HT:PCBM films with different weight PCBM:P3HT ratios 1:0.7, 1:0.8, 1:0.9 and 1:1.

The Atomic Force Microscopy of PEDO:PSS:AuNPs /P3HT:PCBM films with different weight PCBM:P3HT active layer ratios 1:1, 1:0.9, 1:0.8 and 1:0.7, deposited on a Si substrate, as shown in Fig. 5(**a, b, c & d**). The ratio 1: 0.7 film in Fig. 4 (**a**,) exhibit a smooth surface and more uniform in thickness with evidence of phase separation, in which the phase separation is not obvious and the root-mean-square (R.M.S) roughness of the film is 2.11 nm. Fig. 5 (**b, c & d**) show images of surface morphologies of P3HT: PCBM ratios 1:0.9, 1:0.8 and 1:0.7, respectively. It is found that with increasing PCBM concentration, the roughness of the film surface increases, as in ratios 1:0.8 and 1:0.9, as shown in Fig. 5. Besides this at further increase in concentration of PCBM (1:1) large aggregates (domains) of PCBM are observed which is due to percolation of PCBM molecules. On the other hand for concentration of PCBM for 1:1 ratio, the film consists of a homogeneous mixture of P3HT chains and individual PCBM molecules. the R.M.S roughness measured for 1:0.8, 1:0.9 and 1:1 films increased from 3.54, 4.64 and 6.61 respectively. Table 1 summarizes the films' parameters as obtained from AFM image analysis; R_a is the film's mean roughness, R_{max} the maximum height of the film and R.M.S is its root mean square roughness.

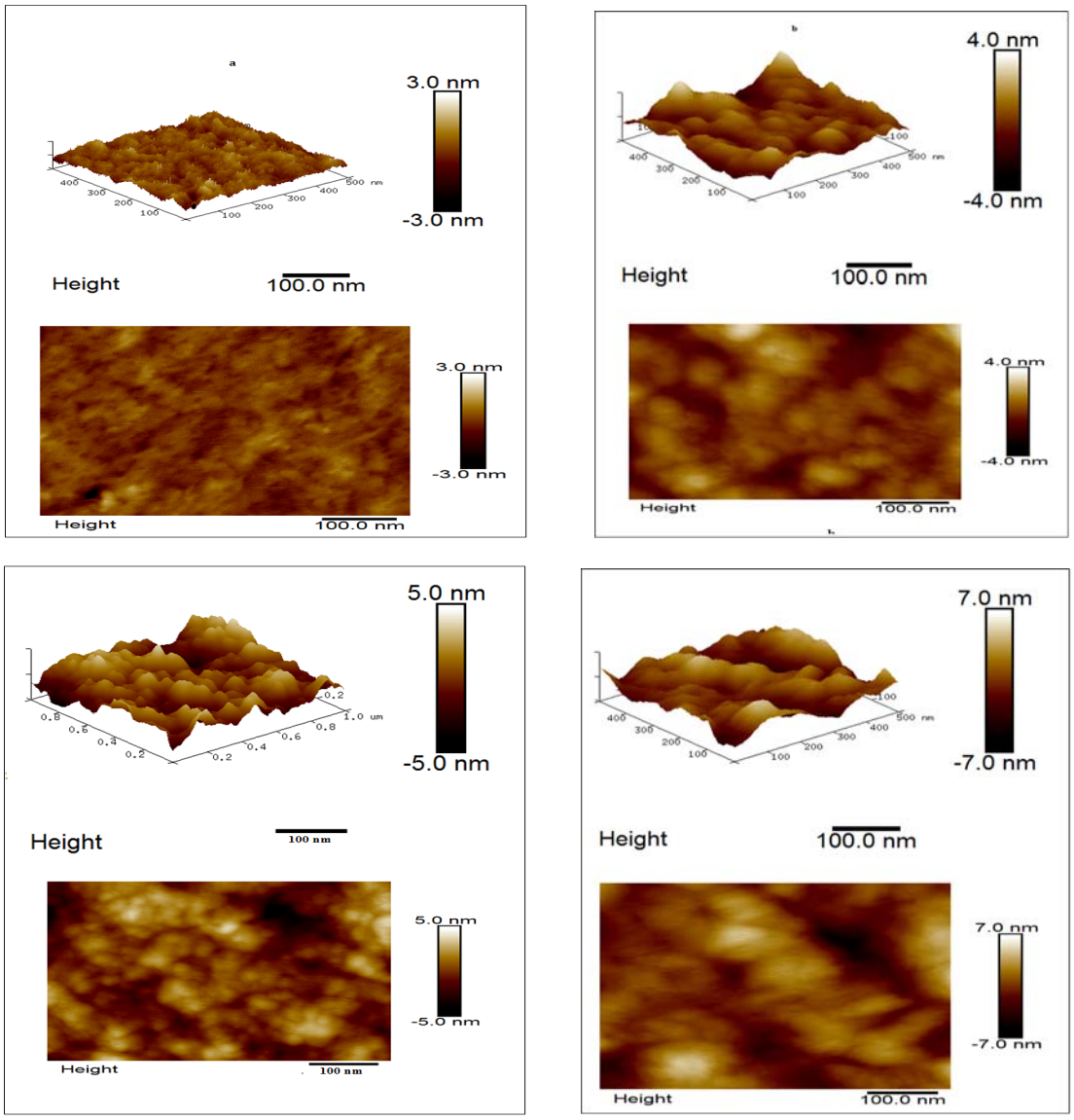

Fig 5: AFM images of PEDOT:PSS:AuNPs/P3HT:PCBM films ratios of (a)1:0.7, (b)1:0.8, (c) 1:0.9 and (d)1:1

Table 1: AFM value for Photovoltaic properties of PEDOT:PSS:AuNPs/ P3HT:PCBM active layer ratios of 1:0.7, (b)1:0.8, (c) 1:0.9 and (d)1:1.

Annealing	R.M.S (nm)	R_a(nm)	R_{max}(nm)
1:0.7	2.11	2.01	16.3
1:0.8	3.54	2.23	20.4
1:0.9	4.64	2.97	35.8
1:1	6.61	3.45	42.6

External quantum efficiency of P3HT:PCBM active layer films with different weight PCBM:P3HT ratios 1:0.7, 1:0.8, 1:0.9 and 1:1., are shown in Fig. 6. The curves of EQE essentially followed the absorption spectrum of the P3HT:PCBM active layer in the range about 350–650 nm corresponding to the absorption wavelength range of P3HT. From quantum efficiency curve it was quite clear that device performance reduced with increase or decrease of the concentration of PCBM acceptor in the P3HT blend. With different PCBM concentration in P3HT, the crystalline structure formation in the blend film varied significantly which affects the device performances. It has been reported that, the concentration of the PCBM clusters and their size were found to be correlated with the amount of PCBM content in the blend [32]. The growth of the PCBM nanocrystals leads to the formation of percolation paths, thereby improving the photocurrent and overall device performance. Above a certain concentration, the PCBM nanocrystals provide mechanical stress on the metal electrode, thereby possibly damaging the interface leading to poorer device performance. Optimization of the composite weight ratio reveals the important role played by morphology for the transport properties of P3HT:PCBM bulk heterojunction based solar cells.

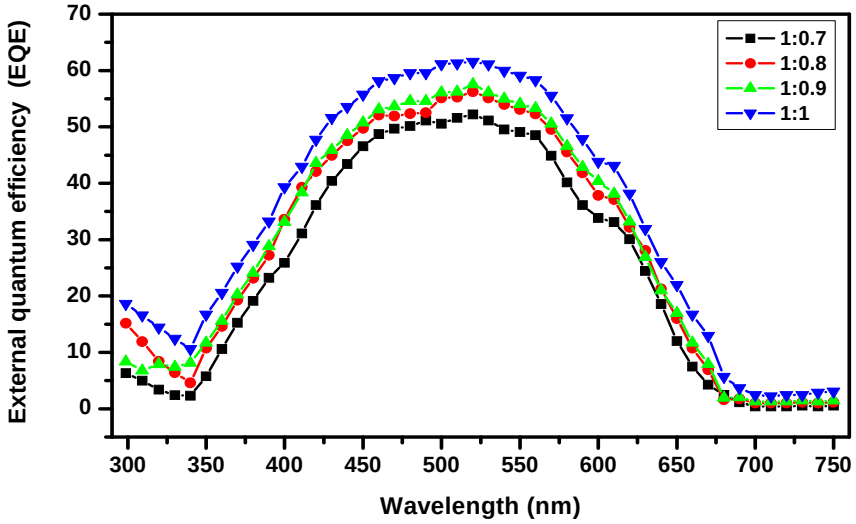

Fig 6: External quantum efficiency (EQE) spectra of PEDO:PSS:AuNPs /P3HT:PCBM films ratios of 1:0.7, 1:0.8, 1:0.9 and 1:1.

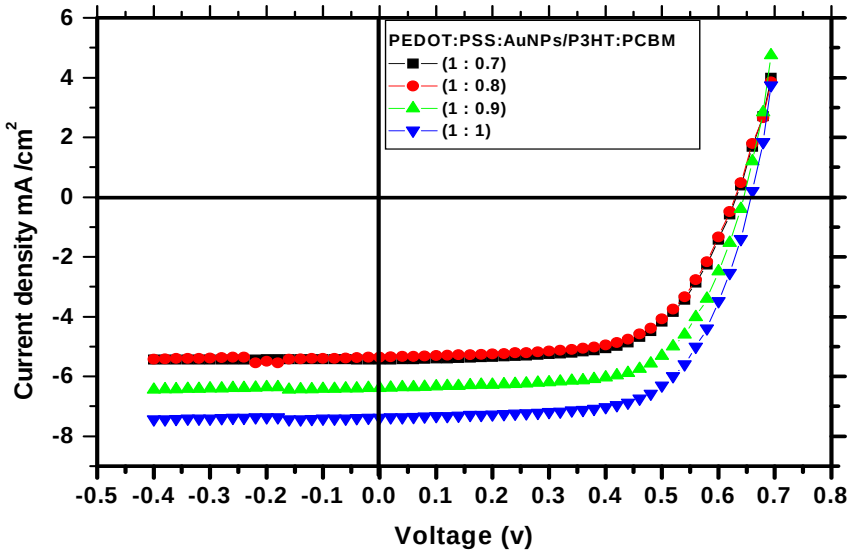

Fig 7: J–V curves of ITO/PEDOT:PSS:AuNPs/P3HT:PCBM/Al active layer ratios of 1:0.7, 1:0.8, 1:0.9 and 1:1.

Current – Voltage (*J-V*) characterization of PEDO:PSS:AuNPs /P3HT:PCBM films, are shown in Fig. 7. Significant improvements show in the J-V characterization results of solar cells, especially on I_{SC}, V_{oc} and FF. While weight ratio of P3HT: PCBM films changing from 1:0.7, 1:0.8,1:0.9 and 1:1. The value of I_{SC} various from 4.2, 4.25, 5.1 and 5.8 mA/cm^2, respectively. However, further increasing of the PCBM content leads to the decreasing of I_{SC}. The V_{oc} values for the weight ratio 1:0.7, 1:0.8,1:0.9 and 1:1 were varying slightly maybe due to the well established ohmic contact between the anode and active layer. The values of V_{oc} are also similar to the previous results 0.49, 0.48 0.51 and 0.52 V, respectively [33]. If both electrodes establish ohmic contacts with the active layer, Voc in these Bulk-Heterojunction cells is related directly to the energy difference between the HOMO level of the donor (P3HT) and the LUMO level of the acceptor (PCBM)

components. The *FF* increases with increasing weight ratio 1:0.7, 1:0.8,1:0.9 and 1:1 from 0.6, 0,61, 0.63, and 0.62. Consequently, the 1:1 weigh ratio composition for blend film gives the highest I_{SC}, V_{oc} and FF, while a blend ratio reduces both of them. As a result, the maximum values of PCE as high as 3.01 is obtained for the structure organic solar cell, using the optimized blend weight ratio of 1:1. While the other values of *PCE* for weight ratio1:0.7, 1:0.8, and 1:0.9 of P3HT: PCBM films changing from 2.06, 2.01 and 2.6, respectively. The increase in PEC of PEDOT:PSS:AuNPs/P3HT:PCBM film can be attributed to the increases in the interfacial contact area between the P3HT:PCBM active layer and PEDOT:PSS:AuNPs intermediate layer, which allowing more efficient hole collection at the anode, and hence increases J_{sc} and *FF*.For the blend material system, it has been established that a fairly homogenous blend is obtained for PCBM contents up to 50% (i.e 1:1) by weight, and that at higher PCBM content, PCBM rich domains begin to segregate [34]. Due to the high electron mobility in PCBM, the PCBM rich domains may assist charge collection in blends, which induce the improvement on device performance. However further increased PCBM content induces a decreasing on the charge carrier collection because of the recombination in the over enlarged PCBM rich domains.

Table 2: Photovoltaic parameters for organic solar cell device with different weight PCBM:P3HT ratios 1:0.7, 1:0.8, 1:0.9 and 1:1.

Devices	V_{oc}(v)	J_{sc}(mA/ cm^2)	FF	PCE(%)
1:0.7	0.62	4.20	0.60	2.06
1:0.8	0.48	4.25	0.61	2.01
1:0.9	0.51	5.1	0.63	2.6
1:1	0.52	5.8	0.62	3.01

4. References

1. Shaheen SE, Radspinner R, Peyghambarian N, Jabboura GE. Fabrication of bulk heterojunction plastic solar cells by screen printing. Applied Physics Letters 2001; 79, 18.
2. Brabec CJ, Sariciftci NS, Hummelen JC. Plastic Solar Cells, Adv. Func. Mater. 11 (2001) 15.H. Spanggaard, F.C. Krebs, A Brief History of the Development of Organic and Polymeric Photovoltaics, Sol. Energy Mater. Sol. Cells 83, 2004, 125.
3. Coakley KM, McGehee MD. Effect of device geometry on the performance of TiO_2 nanotube array-organic semiconductor double heterojunction solar cells. Chem Mater 2004, 16, 4533.
4. Sung-Ho J, Naidu VK, Han-Soo J, Sung-Min P, Jin-Soo P, Sung CK. Optimization of process parameters for high-efficiency polymer photovoltaic devices based on P3HT:PCBM system, 2007; 91(13):1187–1193.
5. Padinger F, Rittberger R, Sariciftci NS. Effects of Postproduction Treatment on Plastic Solar Cells. Adv Funct Mater 2003; 13, 85.
6. Ma W, Yang C, Gong X, Lee K, Heeger AJ. Thermally Stable, Efficient Polymer Solar Cells with Nanoscale Control of the Interpenetrating Network Morphology. Adv Funct Mater 2005; 15, 1617.
7. Li G, Shrotriya V, Huang J, Yao Y, Yang Y. High-efficiency solution processable polymer photovoltaic cells by self-organization of polymer blends. Nat Mater 2005; 4, 864.
8. Reyes-Reyes M, Kim K, Dewald J, Lopez-Sandoval R, Avadhanula A, Curran S, Carroll DL. Meso-structure formation for enhanced organic photovoltaic cells. Org Lett 2005; 7(26):5749-5752.
9. Kim JY, Kim SH, Lee HH, Lee K, Ma W, Gong X, Heeger AJ. New Architecture for high-efficiency polymer photovoltaic cells using solution-based titanium oxide as an optical spacer. Adv Mater 2006; 18, 572.
10. Sirringhaus H, Tessler N, Friend RH. Integrated optoelectronic devices based on conjugated polymers. Science 1998; 280, 1741.
11. Prosa TJ, Winokur MJ, Moulton J, Smith P, Heeger AJ. X-ray structural studies of poly(3-alkylthiophenes): an example of an inverse comb. Macromolecules 1992; 25, 4364.
12. Chirvase D, Parisi J, Hummelen JC, Dyakonov V. Influence of nanomorphology on the photovoltaic action of polymer–fullerene composites. Nanotechnology 2004; 15, 1317.
13. Yohannes T, Zhang FL, Svensson M, Hummelen JC, Andersson MR, Ingana O¨ s. Low-Temperature Combustion-Synthesized Nickel Oxide Thin Films, Thin Solid Films 2004, 449, 152.
14. Van JKJDu, Yang XN, Loos J, Bulle-Lieuwma CWT, Sieval AB, Hummelen JC, Janssen RAJ. Relating the Morphology of Poly(p-phenylene vinylene)/ Methanofullerene Blends to Solar-Cell Performance. Adv Funct Mater 2004; 14, 425.
15. Hoppe H, Niggemann M, Winder C, Kraut J, Hiesgen R, Hinsch A, Meissner D, Sariciftci NS. Nanoscale Morphology of Conjugated Polymer/Fullerene-Based Bulk- Heterojunction Solar Cells. Adv Funct Mater 2004; 14, 1005.
16. Schilinsky P, Asawapirom U, Scherf U, Biele M, Brabec CJ. Influence of the Molecular Weight of Poly(3-hexylthiophene) on the Performance of Bulk Heterojunction Solar Cells. Chem Mater 2005; 17:2175-2180.
17. Kim Y, Cook S, Tuladhar SM, Choulis SA, Nelson J, Durrant JR. A strong regioregularity effect in self-organizing conjugated polymer films and high-efficiency polythiophene: fullerene solar cells. Nat Mater 2006; 5, 197.
18. Brabec CJ, Cravino A, Meissner D, Sariciftci NS, Fromherz T, Rispens MT. Origin of the Open Circuit Voltage of Plastic Solar Cells. Adv Funct Mater 2001, 11, 374.
19. Hou J, Tan Z, He Y, Yang C, Li Y. Synthesis and Photovoltaic Properties of Two-Dimensional Conjugated Polythiophenes with Bi(thienylenevinylene) Side Chains. Macromolecules 2006, 39, 4657.
20. Shrotriya V, Ouyang J, Ricky JT, Gang L, Yang Y. Absorption spectra modification in poly(3-hexylthiophene): methanofullerene blend thin films. Chemical Physics Letters 2005, 411, 138–143.
21. Jilian NF, Messai AM, Manoko M, Willem ALO, Neil JC. Ana Flavia Nogueira, Nanocomposites of gold and poly(3-hexylthiophene) containing fullerene moieties: Synthesis, characterization and application in solar cells. Journal of Power Sources 2012, 215, 99-108.
22. Erb T, Zhokhavets U, Gobsch G, Raleva S, Stühn B, Schilinsky P. Correlation Between Structural and Optical Properties of Composite Polymer/Fullerene Films for Organic Solar Cells. Adv Funct Mater 2005, 15, 1193.
23. Hugger S, Thomann R, Heinzel T, Thurn-Albrecht T. Semicrystalline morphology in thin films of poly(3-hexylthiophene). Colloid Polym Sci 2004, 282, 932.
24. Tsoi WC, James DT, Kim JS, Nicholson PG, Murphy CE, Bradley DDC. The Nature of In-Plane Skeleton Raman

Modes of P3HT ... in P3HT:PCBM Blend Thin Films. J Am Chem Soc 2011; 133:9834–9843.
25. Baibarac M, Lapkowski M, Pron A, Lefrant S, Baltog. SERS spectra of poly(3-hexylthiophene) in oxidized and unoxidized states I. J Raman Spectrosc 1998, 29, 825–832.
26. Amassian A, Pozdin VA L, Smilgies DM, Malliaras GG. Solvent Vapor Annealing of an Insoluble Molecular Semiconductor. J Mater Chem 2010; 20:2623–2629.
27. Gao Y, Grey JK. Resonance Chemical Imaging of Polythiophene/Fullerene Photovoltaic Thin Films: Mapping Morphology-Dependent Aggregated and Unaggregated C=C Species. J Am Chem Soc 2009, 131, 9654-9662.
28. Tsoi WC, James DT, Kim JS, Nicholson PG, Murphy CE, Bradley DDC. The Nature of In-Plane Skeleton Raman Modes of P3HT and Their Correlation to the Degree of Molecular Order in P3HT:PCBM Blend Thin Films. J Am Chem Soc 2011; 133:9834-9843.
29. Louarn G, Trznadel M, Buisson JP, Laska J, Pron AM, Lapkowski SJ. Lefrant, Raman spectroscopic studies of regioregular poly (3-alkylthiophenes). Phys Chem 1996; 100:12532.
30. Huang YC, Liao YC, Li SS, Wu MC, Chen CW, Su WF. Study of the effect of annealing process on the performance of P3HT/PCBM photovoltaic devices using scanning-probe microscopy. Solar Energy Materials and Solar Cells 2009; 93:888–892.
31. Florian M, Silke R, Ning L, Tayebeh A, Christoph JB. Influence of a ternary donor material on the morphology of a P3HT:PCBM blend for organic photovoltaic devices. J Mater Chem 2012, 22, 15570
32. Yasser AMI, Soga T, Jimbo T. Investigation of PCBM Concentration on the Performance of Small Organic Solar Cell. ISRN Renewable Energy 2012, 385415, 8.